robotics

MDPI

Article

Investigation of the Mounting Position of a Wearable Robot Arm

Akimichi Kojima, Dinh Tuan Tran and Joo-Ho Lee *

Graduate School of Information Science and Engineering, College of Information Science and Engineering, Ritsumeikan University, BKC Campus, 1-1-1 Nojihigashi, Kusatsu 525-8577, Shiga, Japan; is0165hp@ed.ritsumei.ac.jp (A.K.); tuan.t.d@ieee.org (D.T.T.)

* Correspondence: leejooho@is.ritsumei.ac.jp

Abstract: In a wearable robot arm, the minimum joint configuration and link length must be considered to avoid increasing the burden on the user. This work investigated how the joint configuration, length of arm links, and mounting position of a wearable robot arm affect the cooperative and invasive workspaces of the overall workspace. We considered the joint configurations and link lengths of passive and active joints in our proposed wearable robot arm, which is called the Assist Oriented Arm (AOA). In addition, we comprehensively studied the position of the arm on the user. As a result, three locations around the shoulders and two around the waist were chosen as potential mounting sites. Furthermore, we evaluated the weight burden when the user mounted the wearable robot arm at those positions.

Keywords: wearable robot arm; wearable positions; passive joints

Citation: Kojima, A.; Tran, D.T.; Lee, J.-H. Investigation of the Mounting Position of a Wearable Robot Arm. *Robotics* **2022**, *11*, 19. https://doi.org/10.3390/robotics11010019

Academic Editor: Marco Ceccarelli

Received: 19 December 2021
Accepted: 25 January 2022
Published: 29 January 2022

1. Introduction

Robot arms have been used as a substitute for human arms in ordinary and precision tasks. As they have become smaller and less expensive, they have been increasingly used in many fields. However, these robot arms are able to move only within the workspace where they have been installed. If work is needed in a different location or over a larger area, another robot arm must be used or the first must be re-installed. Therefore, alternative solutions have been developed, such as a robotic arm on a mobile robot, as proposed by the Mitsubishi Heavy Industries Group [1], or a robotic arm on a drone, as developed by Oonishi et al. [2]. These studies address the disadvantage of robot arms, which is that they are limited to a small workspace. However, it is not easy to introduce these robots into some environments such as factories and agricultural sites. Therefore, wearable robots have been attracting attention. Wearable robot arms have been shown to reduce the burden on a user and improve work efficiency [3,4]. Wearable robot arms have been considered for practical application because they do not need to move autonomously and their cost is low. An example of a practical application of wearable devices is the power suit [5]. Power suits are expected to reduce workloads and assist in the rehabilitation of users such as the elderly. Moreover, wearable robot arms that perform a cooperative task with a user have attracted much attention [6]. Attaching a robot arm to a user enables the user to perform tasks that a single human cannot perform, and it is possible to improve work efficiency. In addition, a wearable robot arm can maintain a certain distance from the user because it is mounted on the user. Therefore, the wearable robot arm can easily support cooperative tasks near the user. Wearable robot arms with these features are expected to be used in the workplace and daily life.

However, two challenges remain in the application of wearable robot arms: the weight burden on the user and the operability of the arm. When dexterity is required in a robot arm, high performance actuators are needed. As a result, the actuators must be high power and heavy. The root joint inevitably needs a heavy actuator because the required output

torque of the actuator increases as it becomes closer to the root joint of the robot arm. Thus, the total weight of the robot arm increases, which increases the burden on the user. In addition, robot arms used in factories are subject to strict regulations such as the prohibition of intrusions into the moving parts of the robot arm and emergency stop devices. This is because if the wearable robot arm is heavy, it could be dangerous. Reducing the weight of wearable robot arm hence increases its safety and practicality.

The "operability" of a wearable robot arm refers to how it is operated when the user's hands are busy. To solve this problem, manipulation methods have been developed, such as [7], which manipulates a robot arm using muscle potential and the "face vector" approach [8], which uses the direction of the user's face to determine the 3D target position. However, irregular movements of the robot arm can be a danger to the user, as Nimawat et al. pointed out in [9], which explained the risk of impact on the user due to user error or misrecognition in the user interface. This risk is caused by the difficulty of operating a robot arm using a user interface when all the joints of the robot arm are dynamically driven.

There are limits to how well the weight and operability problems can be solved in a robot arm mechanism that dynamically drives all joints using actuators. Therefore, we proposed a wearable robot arm called the Assist Oriented Arm (AOA) that is lightweight and safe but retains its operability [10] (Figure 1a). In a conventional wearable robot arm, the angle and force of all joints are controlled by actuators, leading to weight and safety issues. By contrast, joints with different roles were used in the AOA based on the movement of the arm during human work. In humans, the shoulder joint is used to carry the hand to the target workspace before starting the work, and then the tip of the arm is dynamically used to perform the work. The AOA uses a hybrid actuation system that combines two types of joints: active joints that are dynamically driven and passive joints that are directly moved by the user by handling the robot arm. Active joints are driven by actuators in the same way as a conventional robot arm. The passive joint uses a locking mechanism to fix the joint angle, as shown in Figure 1b. A switch mounted on the passive joint turns the locking mechanism on and off. While the switch is pressed, the brake component engages the gear component to lock the angle of the joint. When the switch is released, the lock is released and the joint can be driven freely. Therefore, the joints can be fixed with high torque even with lower power and smaller actuators than before. We performed experiments to evaluate the influence of using the hybrid actuation system in [10] on work efficiency and we were able to reduce the weight of the robot arm without compromising its operability, thus enabling it to be attached to the chest, shoulders, and other attachment positions for assisting with in various tasks.

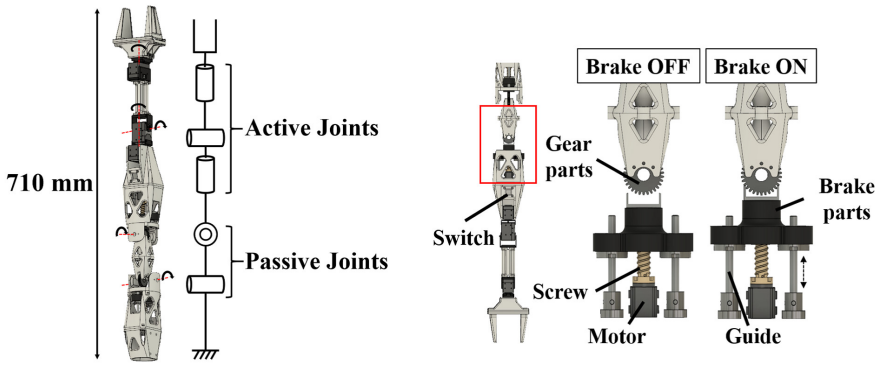

Figure 1. Configuration of previous wearable robot arm.

In this study, the wearable robot arm was optimized for the pick-up task as follows. First, we defined the average human workspace for a wearable robot arm that provides task assistance. Based on the average human workspace, the details of the robot arm were determined. Second, to determine the optimal wearing position for the user, we determined

the wearing position with the widest cooperative workspace between the robot arm and the user. We then selected mounting positions such that the body of the robot arm interferes with the user's hand movement as little as possible. Finally, the robot arm was mounted on subjects at the selected mounting positions, and the position with the least weight burden was determined.

2. Related Work

Several other wearable robot arms have been proposed, and the specifications of each wearing position and the degrees of freedom (DoF) of these existing arms are summarized in Table 1. Baldin et al. [11,12] used a backpack-type attachment device to mount a robotic arm on a user so that it can grasp and support heavy objects on behalf of the user. Stability and balance must be considered in this type of robot arm because it needs to be able to support heavy weights. In addition, Federico et al. [13] modified a previously proposed robotic lower limb [12] to support the user's posture during work. This limb is mounted at the waist and supports the user like a leg. Baldin et al. proposed a wearable robotic arm that is mounted on the shoulder to assist in the installation of ceiling panels [14]. A 5-DoF robotic arm supports the ceiling panel based on the input from an inertial measurement unit sensor attached to the user's hand, leaving the user's hands free to work on the ceiling panel. Vatsal et al. [15] studied a robotic arm that is attached to the elbow and performs tasks in place of a user when both hands of the user are busy. The large size of the workspace is achieved with minimal link length by attaching the robot arm to the user's arm.

Table 1. Features of existing wearable robot arms. MP: mounting position; DoF: degrees of freedom; WS: workspace.

Reference	MP	DoF	Weight	WS
Parietti et al., 2013 [11]	Waist	6	10 kg	Middle
Bonilla et al., 2012 [12]	Waist	6	4 kg	Middle
Parietti et al., 2015 [13]	Waist	3	9 kg	Low
Bonilla et al., 2014 [14]	Shoulder	5	4.5 kg	High
Vatsal et al., 2018 [15]	Elbow	3	2 kg	Middle
Saraiji et al., 2018 [16]	Waist	6	9.6 kg	Middle
Sasaki et al., 2017 [17]	Waist	7	Unknown	Middle

In addition to the above arms, other wearable robot arms that interact with humans have been proposed, such as those by Saraiji et al. [16] and Sasaki et al. [17]. The arm in [16] is a wearable device that integrates a robotic arm and a camera. A remote partner controls the robotic arm attached to the user using a head-mounted display and a controller. The arm in [17] is a 7-DoF robotic arm synchronized with a human leg using motion capture. Because it is synchronized with the user's feet, it can interact intuitively like a third arm. In these cases, the wearable robot arm can perform tasks requiring the same level of dexterity as that of the user. In addition, it is necessary to secure a large workspace for interaction with the user. Therefore, an arm with multiple DoFs (e.g., six DoFs) is required.

These robot arms have different mounting positions and joint configurations because of their different target tasks. Tanaka et al. [18] proposed a framework for the evaluation and design of assistive robots based on the ICF (International Classification of Functioning, Disability, and Health [19]). In this study, the use of the subject's hands was analyzed in

terms of movement frequency using a video recording of daily life obtained by a head-mounted camera. According to [18], 90% of tasks in a person's daily life are "lifting" tasks. In other words, if a wearable robot arm can assist with lifting, 90% of a person's daily tasks can be assisted. They also stated that 90% of the objects lifted are less than 300 g. Therefore, in this study, the objective of the AOA is to lift an object weighing 300 g or less. In this work, only light objects like a cup or pen are lifted. Therefore, the lifting task is called "pick-up". The robot joint configuration and mounting position needed to perform this task are examined in this study.

The position of a wearable robot arm was previously examined in [20] by Nakabayashi et al. They investigated the range of motion obtained by changing the link lengths and joint configurations of the robot arm at three attachment points: the waist, chest, and shoulder. Based on the results, the optimal mounting position and robot arm specifications were obtained by evaluating the coordination and extendability of the user's workspace. They also studied which links of the robot arm can invade the user's workspace. In contrast, this study investigates the joint configuration and link length of a wearable robotic arm with a wide cooperative workspace with the user. As a result, the range of motion is less invasive according to the indexes of cooperativity, extendability, and invasiveness used in [20]. Figure 2 shows the details of extensive workspace, cooperative workspace, and invasive workspace. The main workspace is within easy reach of the user. The extensive workspace Figure 2a is the movable area of the robot hand outside the main workspace. The cooperative workspace Figure 2b is the movable area of the robot hand in the main workspace. The invasive workspace Figure 2c is the range within the main workspace where the body of the robot arm interferes when the robot hand is moved. The following equations define the cooperativeness, extensiveness, and invasiveness indices by [20].

$$V_e = V_h - (V_m \cap V_h) \tag{1}$$

$$V_c = V_m \cap V_h \tag{2}$$

$$V_i = (V_m \cap V_a) - V_c \tag{3}$$

where V_m is the volume of the main workspace, V_e is the volume of the extensive workspace, V_c is the volume of the cooperative workspace, V_i is the volume of workspace invasiveness, V_h is the volume of the robot hand trajectory domain and V_a is the volume of the robot arm trajectory domain. We use the wearable robot arm studied, and select the optimal mounting position.

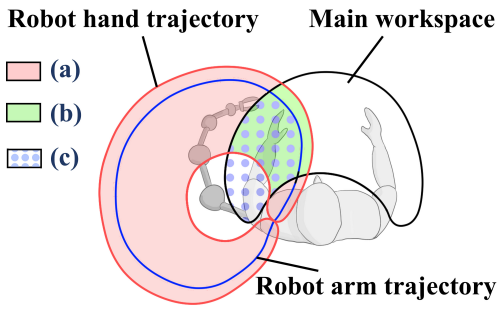

Figure 2. Definitions of each workspace according to [20]: (a) extensive workspace, (b) cooperative workspace, (c) invasive workspace.

3. Workspace Range and Human Body Dimensions

The attachment position of the wearable robot arm depends on the task. As shown in Figure 3a, the user's workspace is classified into three categories, high, middle, and low, based on the acromion point and abdominal position. To define the workspace requirements, we used data from the Life Engineering Research Center [21], which measured the width and depth of the workspace accessible by human movements. These data were used

to determine the average range of motion with respect to the right hand of the subjects. As a constraint, the subject kept the soles of both feet on the ground. Because the data are based on the right acromion point, the range of motion of the left hand was defined using horizontally flipped data. Figure 3b shows the main workspace and extensive workspaces according to these data [21]. The main workspace is the area in which the user can comfortably move their hands. The extensive workspace is the area that the user can reach with difficulty. The National Institute of Advanced Industrial Science and Technology's (AIST) AIST/HQL human body dimensions and shape database [22] was used to obtain the reference dimensions of the human body. In addition, Figure 3c shows the average human body dimensions. These reference data and dimensions were used to study the wearable robot arm's joint configuration, link length, and mounting position.

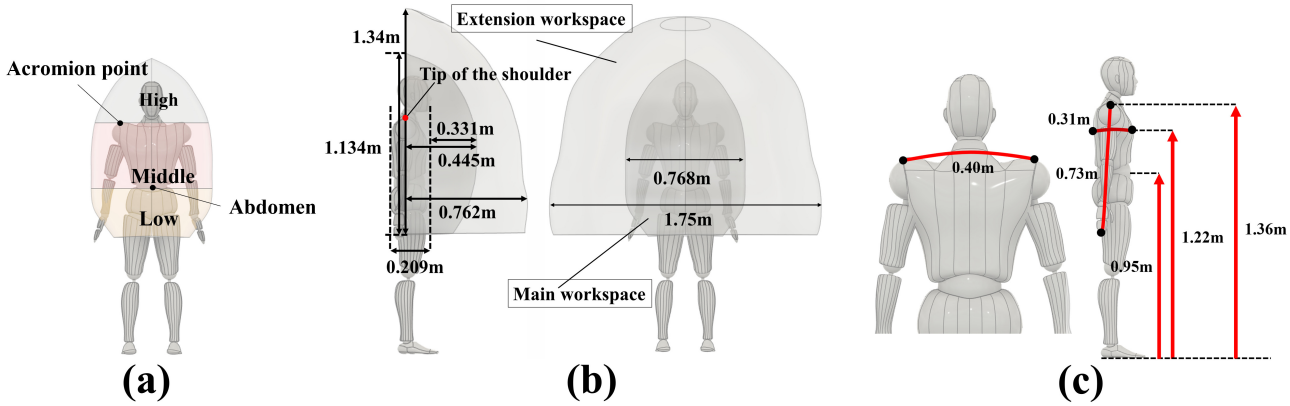

Figure 3. Definitions of the user's workspace and body dimensions: (**a**) Division of the user's main workspace, (**b**) Average workspace range of a person according to [21], (**c**) Human dimensions according to [22].

4. Joint Configuration and Link Lengths of the AOA

The pick-up task described above was used as the target task. Our aim is to determine the best joint configuration and link length in the passive and active joints of the AOA. As shown in Figure 4, the link length from the root position to the first joint of the robot arm is L_1, and the links between subsequent joints are denoted as L_2, L_3, L_{n-1}, and L_n. The rotation axes of the joints are expressed using pitch, yaw, and roll. The link lengths and joint configurations of the robot arm are studied using kinematics. Using the Denevit-Hartenberg representation of Figure 5, the transformation between the reference frame $i-1$ and the reference frame i can be easily calculated by the following Equation (4).

$$ {}^{i-1}T_i = \left[\begin{array}{ccc|c} \cos\theta_i & -\sin\theta_i\cos\alpha_i & \sin\theta_i\sin\alpha_i & a_i\cos\theta_i \\ \sin\theta_i & \cos\theta_i\cos\alpha_i & -\cos\theta_i\sin\alpha_i & a_i\sin\theta_i \\ 0 & \sin\alpha_i & \cos\alpha_i & d_i \\ \hline 0 & 0 & 0 & 1 \end{array}\right] \quad (4) $$

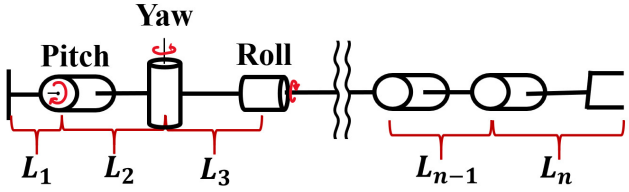

Figure 4. Definition of the joint configurations.

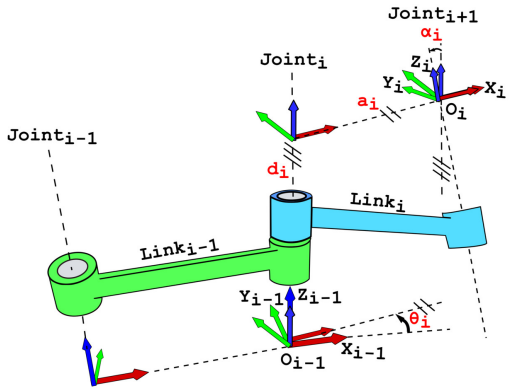

Figure 5. Denavit-Hartenberg represenation.

4.1. Passive Joint

In a passive joint, the joint angle lock is turned on and off by a switch attached to the body of the robot arm, and the user moves the hand to the target workspace while holding the robot arm. The switch should be placed in a position that is easy for the user to reach and press, and it should not be affected by the joint angle or posture of the robot arm. If the switch is mounted on the link of the active joint, it is difficult for the user to press the switch because the posture of the robot arm can change substantially before and after an operation. In a passive joint, the posture of the joint does not change during the operation, and it is appropriate to implement the switch on the link of the passive joint.

The maximum range of the passive-joint links should remain within the area that the user can easily reach. However, the range of motion of the robot arm varies depending on their length. Figure 6 shows the change in the range of motion of the robot hand when the length of the passive joint is changed. When calculating the range of motion, the active joints were assumed to be constant. In addition, the angles of these joints' angles were varied from 90° to −90°. As shown in Figure 6a, if the links extend beyond the main working range, the range of motion of the robot arm increases, but the range of coordination in the user's main workspace decreases. In Figure 6b, the lengths of the passive-joint links are short, and the overall range of motion of the robot arm is narrow. Moreover, the cooperative workspace is wide, but the extensive workspace is narrow. In Figure 6c, the link length of the passive joint is set to equal the user's reach. In this case, there is no bias in the cooperative and extensive workspace, and the switch to turn the lock on and off can be located within arm's reach of the user. Therefore, when the robot arm is mounted on the front of the user, the total length of the passive-joint links should be 0.33 m from the front of the user to the main workspace, according to the dimensions in Figure 3b. When mounting the prototype of the AOA, a gap of about 0.05 m is required for the vest and the fixed parts of the robot arm. Therefore, L1 requires 0.05 m, and the preferred total length of the passive-joint links for L2 and L3 is 0.28 m.

Next, we consider the configuration of the passive joint. The aim of the passive joint is to move the robot arm's hand to the workspace. In addition, because it is mounted on a human, it is necessary to minimize the joint configuration to consider weight and safety. The minimum number of DoF to move the tip of the robot arm in three dimensions is two. Of the three rotation axes roll, pitch, and yaw, roll-pitch and roll-yaw are combined when the roll rotation is placed at the root position. However, both combinations have the same range of motion. The configuration in which roll rotation is provided at the tip of the robot arm should be excluded because it is movable only in two dimensions. We consider a joint configuration and a link length that can move widely within the user's main work range. In this case, the central position of the body is used to maximize the cooperative workspace of the robot arm and the user. The center position of each height range shown in Figure 3 (high, middle, and low) is selected as a mounting position. We then compare the range of the passive joint using these three mounting positions for a maximum link length of the passive joint of 0.28 m, and various lengths of L_2 and L_3 in steps of 0.01 m. We considered

the joint configuration, which is wider in the work envelope of the wearable robot arm within the user's workspace.

Figure 7 shows the maximum cooperative workspace for each joint configuration by using kinematics. The red area in Figure 7 shows the range of motion of the passive joints within the user's main workspace. A roll-pitch configuration has a narrower range than pitch-yaw and yaw-pitch configurations because it moves in a hemisphere around the pitch rotation axis. In addition, the work envelopes of the pitch-yaw and yaw-pitch configurations are similar, but the cooperative workspaces are different. Figure 8 compares the work envelope of the passive joint when it is mounted in the high, middle, and low positions for each joint configuration. In all three positions, the pitch-yaw configuration has a wide range of motion within the user's main workspace. In the relationship between link length and work envelope, the work envelope is widest when L_2 is 0.03 m and L_3 is 0.25 m. Therefore, these values were used. Table 2 lists the specifications of the passive joints. Table 3 shows the DH parameters from the root to the tip of the passive joint. Based on these parameters, the equation for tip of passive joints is shown below.

$$ {}^{0}T_3 = {}^{0}T_1 {}^{1}T_2 {}^{2}T_3 = \begin{bmatrix} \cos\theta_1 \cos\theta_2 & -\cos\theta_1 \sin\theta_2 & \sin\theta_1 & \cos\theta_1 (l2 + l3 \cos\theta_2) \\ \cos\theta_2 \sin\theta_1 & -\sin\theta_1 \sin\theta_2 & -\cos\theta_1 & \sin\theta_1 (l2 + l3 \cos\theta_2) \\ \sin\theta_2 & \cos\theta_2 & 0 & l1 + l3 \sin\theta_2 \\ 0 & 0 & 0 & 1 \end{bmatrix} \quad (5) $$

These link lengths and joint configurations were used to study the joint configurations and link lengths of the active joints in this research.

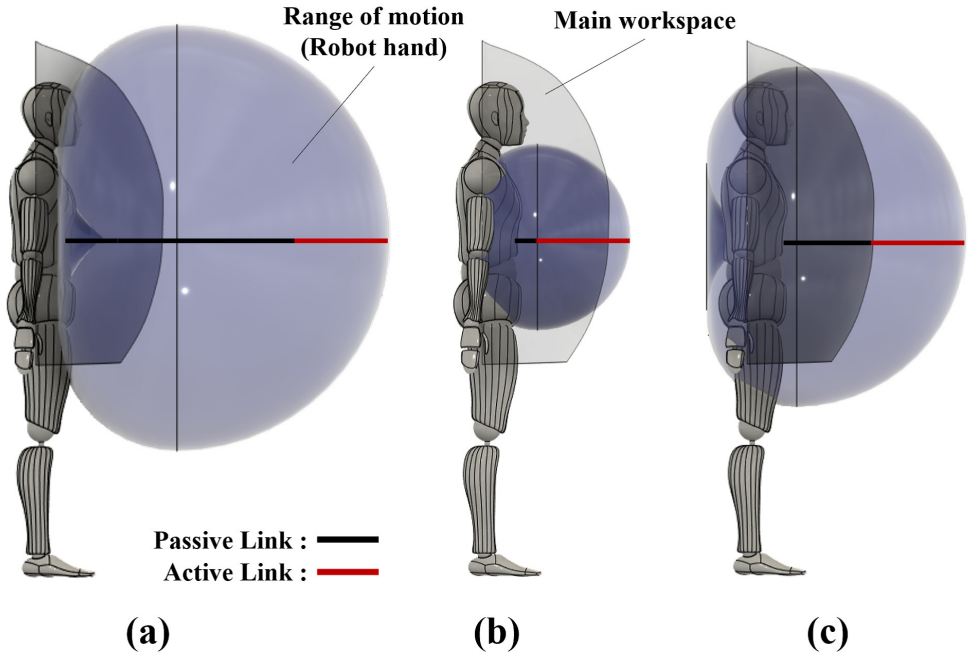

Figure 6. Effect of passive-joint link length on the range of motion when the link length is (**a**) greater than the main workspace, (**b**) much smaller than the main workspace, and (**c**) similar to the maximum main workspace.

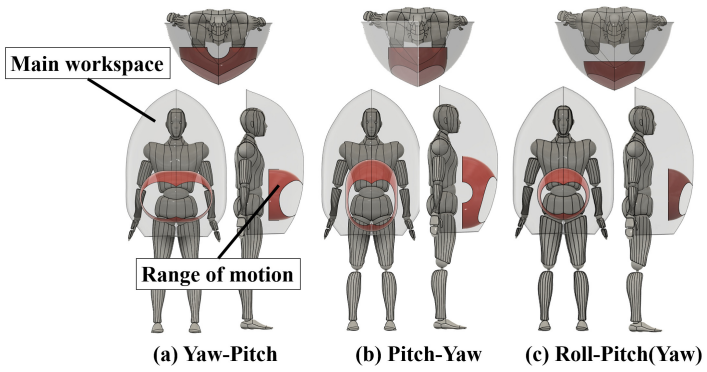

Figure 7. Maximum range of motion for each passive joint configuration.

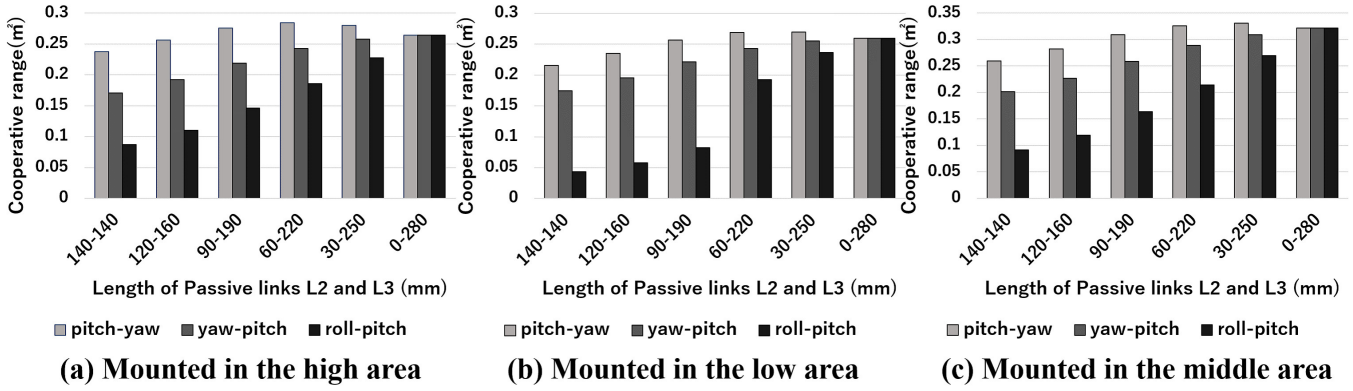

Figure 8. Differences in the range of motion of passive joint configurations and link lengths at the high, middle, and low positions.

Table 2. Passive joint specifications considered.

Joint Configuration	Range of Motion	L_1	L_2	L_3
Pitch-Yaw	Pitch: $-90° < \theta < 90°$ Yaw: $-90° < \theta < 90°$	0.05 m	0.03 m	0.25 m

Table 3. DH parameter for the passive joints.

i	θ	d	a	α
1	0	l1	0	0°
2	θ_1	l2	0	90°
3	θ_2	l3	0	0°

4.2. Active Joint

Active joints are used for dynamic movements that cannot be achieved with passive joints alone. We consider the joint configurations and link lengths required for the dynamic pick-up task. The configuration of the active joint depends on the target task. For example, when the posture of an object needs to be controlled in three dimensions, the number of

DoFs required for the joints increases. However, a wearable robot arm is mounted on a user. Therefore, the position of the robot arm can change because of the user's movement. Wearable robotic arms are better suited for lifting and moving objects than for detailed dexterous tasks. Because the weight of the robot arm increases as the number of DoFs increases, it is necessary to minimize the joint configuration and passive joints. In the workspace of the active joint, cooperative and extensive workspaces are required. The cooperative workspace is the overlap in the ranges of motion between the robot arm and the user's arms. The extensive workspace is the area in the workspace that is outside the cooperative workspace. In some cases, the extensive workspace is essential, for example, in a task where a user uses lights in the extensive workspace that dynamically illuminate the workspace. In such a task, if the active joint holding the light is within the cooperative workspace, this would interfere with the user's hand and affect the work. An example of a cooperative area task is when the robot arm holds an object within the cooperative workspace, such as during soldering. It is necessary to consider the DoFs and link length to keep both workspaces in balance.

The requirements for active joints are a wide range of motion and minimal posture control when grasping an object. The joint arrangement of a typical robot arm is shown in Figure 9. In the case of Figure 9a–c, the range of motion is a line or plane, which greatly limits the tasks that can be performed. In the case of Figure 9d,e in the figure, more movements are possible compared to Figure 9a–c because they are movable in three dimensions. However, the tasks such as pickup and manipulation require more than 4DoF because of necessary for attitude control of the end-effector. For the object lifting task, which is the objective of this research, Figure 9a–e can also perform the task. However, lifting objects commonly used in daily life, such as cups and cables, requires a three-dimensional range of motion and posture control of the end-effector. Therefore, in this study, we use the joint configuration shown in Figure 9d,e.

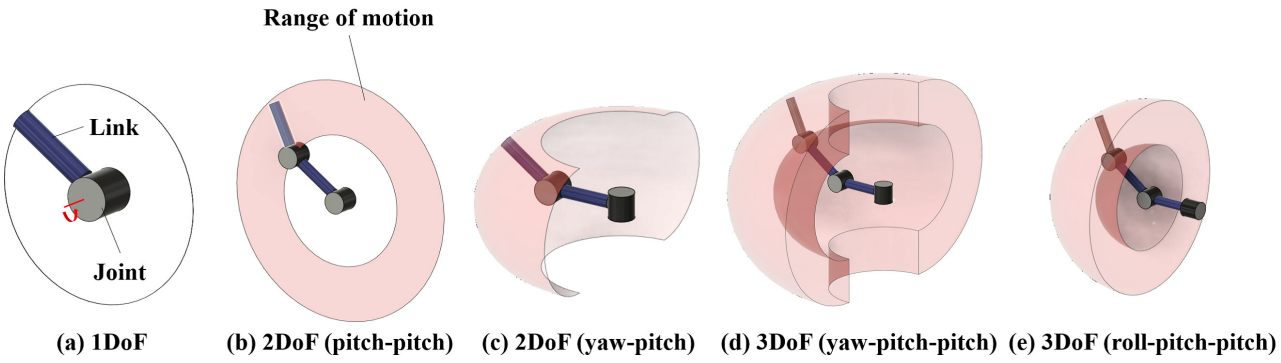

Figure 9. Joint configuration of the robot arm.

For active joints, the longer the link length, the wider the range of motion. However, the longer the link length, the greater the burden on the user. If the maximum link length of an active joint is set to be longer than the extensive workspace shown in Figure 3b, the range of motion becomes wider, but the range of motion becomes excessive, resulting in a greater burden on the user. In addition, if the maximum link length of the active joint is too short, the range of motion becomes narrow and the coordination and extensibility become low. Therefore, we set the length of the active joint to 0.317 m, which is the maximum extensive workspace, to ensure the maximum cooperative and extensive workspace between the user and the robot arm. In the case of Figure 9d, the robot arm can move in three dimensions, but three joints need to be placed on the active joint link. The maximum link length of the active joint is limited, and a large number of joints would conversely reduce the range of motion. However, in the case of Figure 9e, by placing the root-roll joint on the link of the passive joint, a wide range of motion can be achieved without putting pressure on the range of motion of the active joint. In addition, the installation of the roll rotation on the link of the passive joint does not reduce the range of motion of the passive joint.

Therefore, a roll-pitch-pitch joint configuration was adopted. Roll-yaw-yaw is the same as roll-pitch-pitch by rotating 90° in the roll direction. A roll joint is provided at the end of the active joint for minimum posture control of the end-effector, and four degrees of freedom (roll-pitch-pitch-roll) have used. Thus, we achieve the minimum posture control required for grasping and lifting an object.

In the multiple joints on the same rotation axis, the range of motion varies depending on the link length between the joints. Therefore, we solved the kinematics using the parameters in Table 4 and calculated the range of motion using the following equation.

$$^{0}T_{7} = {}^{0}T_{1}{}^{1}T_{2}{}^{2}T_{3}{}^{3}T_{4}{}^{4}T_{5}{}^{5}T_{6}{}^{6}T_{7} \quad (6)$$

As shown in Figure 10, where the gray line shows the percentage of the work envelope that is also cooperative workspace, and the black line shows the range of motion of the wearable robot arm. Moreover, joint intervals of 0.13 m yield the broadest range of motion. However, the percentage of the cooperative workspace in the work envelope is small. With a link length of 0.073 m, it is possible to ensure the broadest range of motion while retaining a large cooperative workspace. The specifications of the active joints considered in this study are listed in Table 5. The joint configuration and link lengths of the active joints (Table 5) and passive joints (Table 2) were used to study the optimal wearing position for user.

Table 4. DH parameter for overall robot arm.

i	θ	d	a	α
1	0	l1	0	0°
2	θ_1	l2	0	90°
3	θ_2	0	0	90°
4	θ_3	0	l3	90°
5	θ_4	l4	0	0°
6	θ_5	0	0	90°
7	θ_6	0	l5	0°

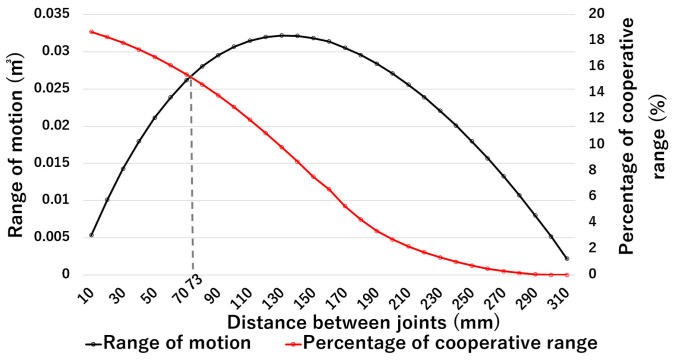

Figure 10. Range of motion due to the difference in the link lengths of the active joints.

Table 5. Specifications of the active joints in the wearable robot arm.

Joint Configuration	Range of Motion	L_4	L_5
Roll-Pitch-Pitch	Pitch: $-90° < \theta < 90°$ Roll: $0° < \theta < 360°$	0.073 m	0.244 m

5. Mounting Position

5.1. Selection of the Mounting Position

When selecting the mounting position, the weight of the robot arm must be considered. The total weight of the AOA prototype is 1.2 kg. Therefore, when it is mounted on the upper arm or elbow, it places a heavy burden on the user, as described in Mandinei et al. [23]. The load could be carried on the head, as studied in [24] by Lloyd et al. However, this configuration is not appropriate for use with a robot arm that can change its center of gravity. Therefore, we evaluated positions that range from the shoulder area to under the abdomen. In the lower part of the body, the area that ranges from the abdomen to the inseam position was evaluated.

5.2. Mounting Position Evaluation

Depending on the attachment position of the robot arm, the link of the wearable robot arm can interfere with the user's arm when the user performs work. It is not sufficient to determine the attachment position based on the size of the cooperative workspace in the work envelope. Therefore, it is necessary to consider the attachment position that avoids the places where the invasive workspace is significant within the user's main workspace. We analyzed the cooperative and invasive workspace at the three locations of high, middle, and low, as shown in Figure 3a. The high, middle, and low areas are 0.038 m^3, 0.093 m^3, and 0.053 m^3 in size, respectively. If the invasiveness in the middle range is high, the robot arm will interfere with the user's hand and affect the work.

When the robot arm is mounted in the middle of the body, it has a wide cooperative workspace at any height. Figure 11a shows the ratio of cooperative workspace to invasive workspace in the entire user's main workspace. When the robot arm is mounted at the middle positions, the cooperative workspace is large, but the range of motion in the user's arm is affected because the invasive workspace is also large. When the robot arm is mounted at the low positions, the invasive workspace can be wide depending on the mounting position, but the percentage of invasive workspace decreases as the mounting position approaches the acromion point. However, Figure 11a shows that the cooperative workspace of the entire main workspace is as low as 65% at the attachment position with the smallest invasive workspace. Figure 11b presents the results for the middle and low ranges only, rather than the entire main workspace. The horizontal axis shows the percentage of the invasive workspace within the middle range, and the vertical axis shows the percentage of the cooperative workspace within the middle and low ranges. In the middle and low ranges, the cooperative workspace is 81% in the mounting position with the smallest invasive workspace. These mounting positions are suitable for supporting work in the middle and low ranges. Next, the mounting position in the shoulder area was examined. Figure 11c shows the distribution in the percentage of cooperative workspace within the high and middle ranges. The invasive workspace within the middle range at the selected mounting position of the shoulder position is also shown. The percentage of the cooperative workspace within the high and middle ranges is higher than that when the arm is worn in the low range because it is less invasive in the middle range. In addition, mounting the device around the shoulder is optimal for cooperative work in the high and middle ranges. Figure 12 shows the candidate mounting positions obtained as a result of the study. The positions in the low range have an invasive workspace within the middle range of 80% or less and a cooperative workspace within the low and middle ranges of 80% or more.

The shoulder attachment positions have an invasive workspace within the middle and high ranges of 60% or less and a cooperative workspace within the middle range of 80% or more. These mounting positions were designed to be more cooperative and less invasive for the user. It is also necessary to consider the weight burden on the user at these mounting positions.

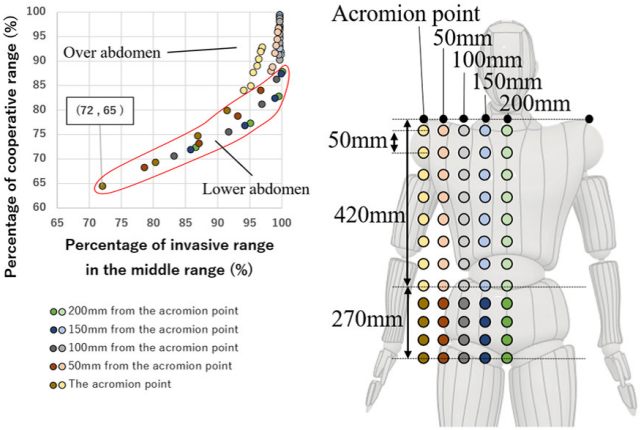

(a) Percentage of cooperative workspace in the total main workspace and percentage of invasive range in the middle range.

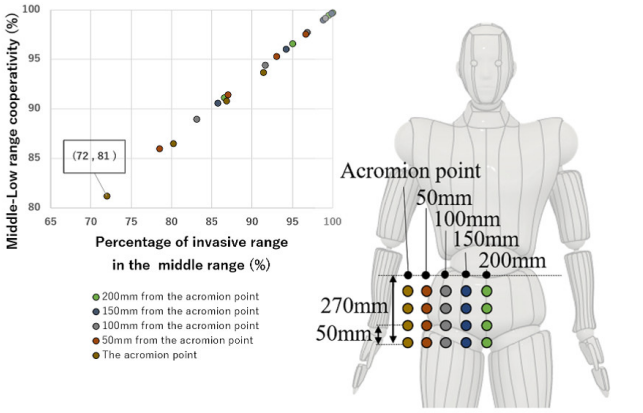

(b) Lower body mounting position: Percentage of cooperative workspace in the middle and low ranges and percentage of invasive range in the middle range.

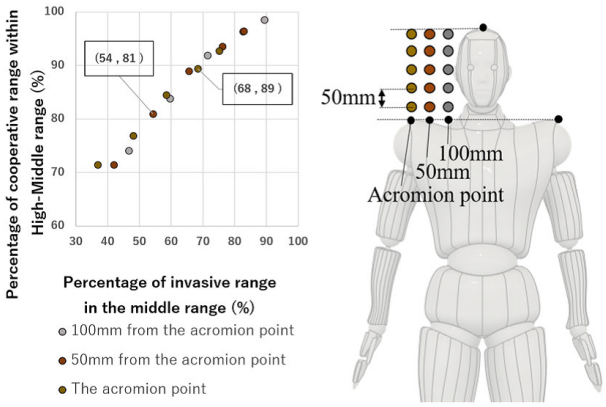

(c) Shoulder body mounting position: Percentage of cooperative workspace in the middle and high ranges and percentage of invasive range in the middle range.

Figure 11. Percentage of cooperative workspace in the main workspace and invasive workspace in middle range.

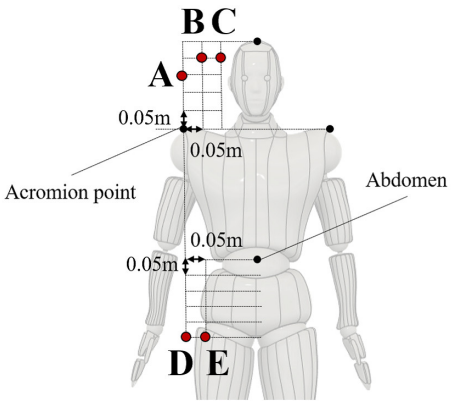

Figure 12. Candidates of mounting positions.

5.3. Evaluation of the Stress on the Body

Anderson et al.'s study [25] evaluated the burden of weight on the front of the body when the user is standing and walking. They found that the burden on the user decreased when the arm was mounted on the waist because the muscle must more actively support the robot arm on the shoulder than on the waist. In Abe et al.'s study [26], the burden of carrying weight on the back was evaluated in terms of energy cost. When comparing the load generated by mounting the arm on the upper and lower back, significantly lower energy costs were identified when the load was placed on the upper back. Therefore, the robot arm is fixed to the top of the back using aluminum links and steel plates.

The stresses on the body were compared when the robot arm was attached to the position shown in Figure 12. Figure 13 shows the stress when the robot arm is attached. For the simulation, Fusion 360 for stress analysis simulation function was used. 3D models of the aluminum links and plates that hold the robot arm in top of the back, the vest, and the user's body were fabricated, and simulations were performed to take into consideration the effects of contact between the models. The vest is attached by belts on both shoulders and abdomen. Therefore, the load of wearing the robot arm is transmitted to the user's body through the belt of the vest. The tip of the aluminum links in Figure 13 indicates the position of the center of gravity of the robot arm. We evaluated the stress on the user's body when the weight of the robot arm was added to the center of gravity position. Figure 13a–c show the stresses in the robot arm at the shoulder mounting positions A, B, and C. When a force is applied to the tip of the aluminum link, the moment of pulling the vest back causes large stresses in the user's abdomen and upper back. Figure 13d,e show the stresses when the robot arm is attached to the waist positions D and E. We compared to the case where the robot arm is attached to the shoulder position, the stress in the abdomen is smaller, and the stress due to the steel plate is generated in a wide area of the back. Based on the stress evaluation results, we had the subjects mount the robot arm to evaluate the weight burden.

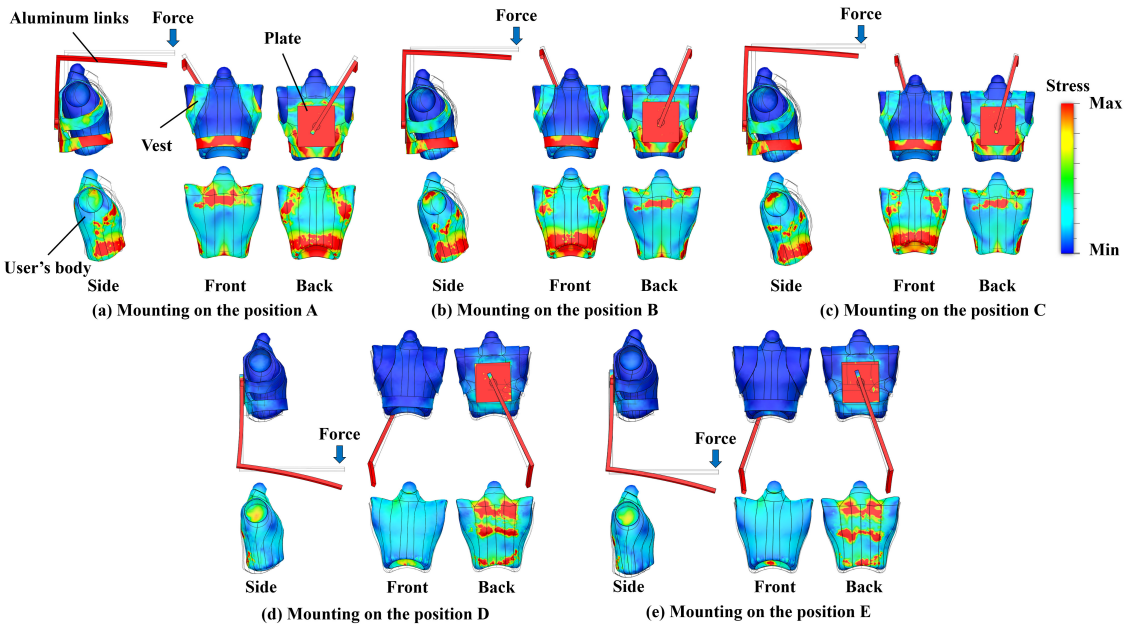

Figure 13. Stress verification at each mounting position.

5.4. Evaluation and Discussion

In order to study the weight burden on the user, we conducted an evaluation using candidate mounting locations. The implemented AOA is shown in Figure 14, where a locking mechanism is attached to the passive joint. We considered the size of the locking mechanism; it is necessary to move the position of the rotation axis in parallel in order to have a link length of 0.03 m. The robot arm was fixed to the back using a harness

(Figure 14). The harness can be adjusted to the height and angle of the robot arm. The waist position was fixed in the same way (Figure 14). In the experiment, the AOA was mounted on the subject for 1 min and the user burden was evaluated for each wearing position with a 20-minute rest. In addition, the wearing positions was randomized. A questionnaire survey was conducted after the experiment using a five point Likert scale for each wearing position. The subjects were eight males in their twenties. The degree of the burden felt at mounting positions A to E was rated on a scale of 1 to 5, with 1 being the least burdensome and 5 being the most burdensome.

The results of the evaluation experiment are shown in Figure 15, where the horizontal axis of the graph is the mounting positions A to E. The vertical axis is the evaluated value of the user's burden, where 1 indicates a light burden and 5 indicates a heavy burden. The shoulder positions of A, B, and C are more burdensome positions than the waist positions of D and E. A two-tailed t-test was conducted at a significance level of 5% for the mounting positions A, B, and C. The p-value results were 0.73 for A and B, 0.14 for B and C, and 0.08 for A and C, which are all greater than 0.05. Thus, there were no significant differences among these positions. The two-tailed t-test was also performed at a significance level of 5% for mounting positions D and E. The p-value was 0.63, so again, there was no significant difference. The comparison of the waist and shoulder positions showed a significant difference because the p-value for wearing positions C and E was 0.006. In other words, it is easier for the user to wear the device at the waist than at the shoulder. When the robot arm is mounted on the shoulder, many users commented that they felt uncomfortable because the robot arm was visible in the user's peripheral vision. There is almost no difference in the ratio of cooperative to invasive workspace between the shoulder and the waist, but it is more appropriate to attach the device to the waist considering the user burden. Figure 16a shows an example of taping a cable. The taping process can be performed using both hands while supporting the end of the cable with the robot arm. Figure 16b is an example of fixing a board. While supporting the board with the robot arm, the board can be fixed using a drill. By attaching the robot arm to the considered mounting position, it can be applied as a wearable robot arm with elasticity, cooperativity, and invasiveness.

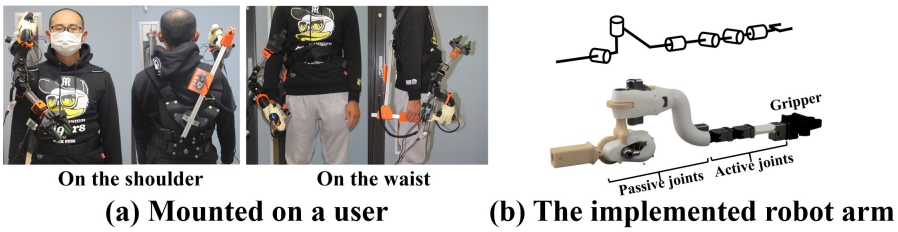

Figure 14. Wearing AOA on the shoulder and waist. The AOA was implemented based on the dimensions specified in this study.

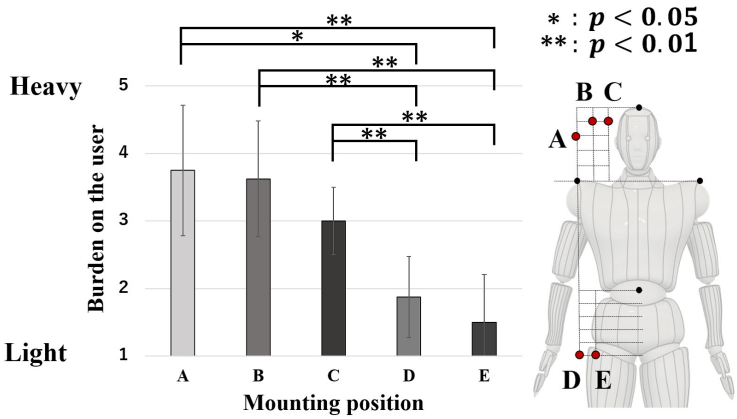

Figure 15. Results of the user burden experiment.

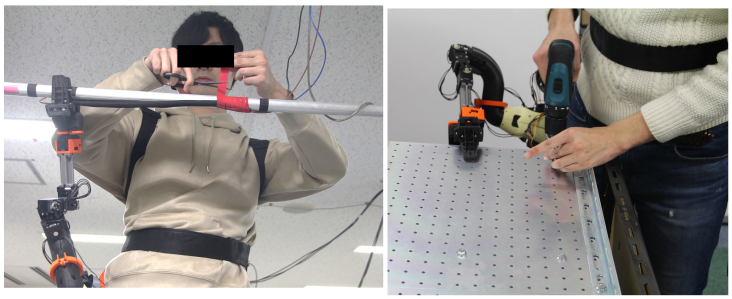

(a) Cable taping task **(b) Plate fixing task**

Figure 16. Applications of the wearable robot arm.

6. Conclusions

In contrast to an industrial robot arm, a wearable robot arm does not need all of its joints to be controlled by actuators. A combination of passively driven passive joints and dynamically driven active joints was considered in this study to reduce the weight and increase the safety of a wearable robot arm. This study investigated the optimal configuration of DoFs, link length, and mounting position for the wearable robot arm. The mounting position on the user was selected based on average human body dimensions and average range of motion of the arms. The optimal mounting position was determined based on the ratio of the cooperative workspace to the invasive workspace. Because the wearable robot arm is mounted on the user, the operating range can be tailored to the user's task. This approach also has a significant advantage in that it can provide a wide cooperative workspace. In recent years, wearable robotic arms have been widely studied, and each wearable robotic arm has been considered in various wearing positions. It is not easy to generalize which mounting position is best because the optimal position varies depending on the work and the DoFs of the robot arm. However, the wearable robot arm considered in this paper was studied based on the joint configuration, link length, and wearing position. This arm is needed to perform the lifting task, which accounts for 90% of daily tasks. Lifting is a task that can be applied not only in daily life but also in various fields such as factories and agriculture. Therefore, the investigations made in this paper will contribute to the generalization of wearable robot arms. If the wearing position is standardized, it will be possible to compare wearable robot arms, which is difficult at present, and better wearable robot arms can be considered. The future work of this research will be to develop and study a user interface for task support based on the lifting task using the wearable robot arm AOA.

Author Contributions: Conceptualization, A.K. and J.-H.L; methodology, A.K.; software, A.K.; validation, A.K., D.T.T. and J.-H.L.; formal analysis, A.K.; investigation, A.K.; resources, A.K.; data curation, A.K.; writing—original draft preparation, A.K.; writing—review and editing, A.K., D.T.T. and J.-H.L.; visualization, A.K.; supervision, J.-H.L.; project administration, D.T.T. and J.-H.L.; funding acquisition, J.-H.L. All authors have read and agreed to the published version of the manuscript.

Funding: This work was funded by the Ritsumeikan Global Innovation Research Organization.

Institutional Review Board Statement: Not applicable.

Informed Consent Statement: Informed consent was obtained from all subjects involved in the study.

Data Availability Statement: AIST/HQL 3D Anthropometric Database 2003 at https://www.airc.aist.go.jp/ (accessed on 18 December 2021). HQL Database for Human Life Engineering at https://www.hql.jp/database/ (accessed on 18 December 2021).

Conflicts of Interest: The authors declare no conflict of interest.

References

1. Leona, M.; Hashimoto, T.; Shimonabe, N.; Yano, M.; Onitsuka, H.; Fujita, J. Development of the Remote Decontamination Robot 'MHI-MEISTeR II' for an Upper Floor of Reactor Building in Fukushima Daiichi NPP. *E-J. Adv. Maint.* **2017**, *9*, 126–131.
2. Ohnishi, Y.; Takaki, T.; Aoyama, T.; Ishii, I. Development of a 4-Joint 3-DOF Robotic Arm with Anti-reaction Force Mechanism for a Multicopter. In Proceedings of the 2017 IEEE/RSJ International Conference on Intelligent Robots and Systems (IROS), Vancouver, BC, Canada, 24–28 September 2017.
3. Jo, I.; Bae, J. Design and Control of a Wearable Hand Exoskeleton with Force-controllable and Compact Actuator Modules. In Proceedings of the IEEE International Conference on Robotics and Automation (ICRA), Seattle, WA, USA, 26–30 May 2015; pp. 5596–5601.
4. Kern, N.; Schiele, B.; Schmidt, A. Multi-sensor Activity Context Detection for Wearable Computing. In Proceedings of the European Symposium on Ambient Intelligence, Veldhoven, The Netherlands, 3–4 November 2003; pp. 220–232.
5. Kawamoto, H.; Sankai, Y. Power Assist System HAL- 3 for Gait Disorder Person. In Proceedings of the International Conference on Computers for Handicapped Persons 2002, Linz, Austria, 15–20 July 2002; pp. 196–203.
6. Khodambashii, R.; Weinberg, G.; Singhose, W.; Rishmawi, S.; Murali, V.; Kim, E. User Oriented Assessment of Vibration Suppression by Command Shaping in a Supernumerary Wearable Robotic Arm. In Proceedings of the IEEE-RAS 16th International Conference on Humanoid Robots (Humanoids), Cancun, Mexico, 15–17 November 2016.
7. Morizono, T.; Tahara, K.; Kino, H. Choice of Muscular Forces for Motion Control of a Robot Arm with Biarticular Muscles. *J. Robot. Mechatron.* **2019**, *31*, 143–155.
8. Iwasaki, Y.; Iwata, H. A Face Vector—The Point Instruction-type Interface for Manipulation of an Extended Body in Dual-task Situations. In Proceedings of the International Conference on Cyborg and Bionic Systems, Shenzhen, China, 25–27 October 2018; pp. 662–666.
9. Nimawat, D.; Raj, P.; Jailiya, S. Requirement of Wearable Robots in Current Scenario. *Eur. J. Adv. Eng. Technol.* **2015**, *2*, 19–23.
10. Kojima, A.; Yamazoe, H.; Lee, J.-H. Wearable Robot Arm with Consideration of Weight Reduction and Practicality. *J. Robot. Mechatron.* **2020**, *32*, 173–182.
11. Parietti, F.; Asada, H.H. Dynamic Analysis and State Estimation forWearable Robotic Limbs Subject to Human-Induced Disturbances. In Proceedings of theIEEE International Conference on Robotics and Automation (ICRA), Karlsruhe, Germany, 6–10 May 2013; pp. 3880–3887.
12. Llorens-Bonilla, B.; Parietti, F.; Asada, H. Demonstration-Based Control of Supernumerary Robotic Limbs. In Proceedings of the IEEE International Conference on Intelligent Robotics and Systems 2012, Portugal, 7–12 October 2012; pp. 3936–3942.
13. Parietti, F.; Chan, K.C.; Hunter, B.; Asada, H.H. Design and Control of Supernumerary Robotic Limbs for Balance Augmentation. In Proceedings of the IEEE International Conference on Robotics and Automation (ICRA), Seattle, WA, USA, 26–30 May 2015; pp. 5010–5017.
14. Llorens-Bonilla, B.; Asada, H.H. A Robot on the Shoulder: Coordinated Human-Wearable Robot Control Using Coloured Petri Nets and Partial Least Squares Predictions. In Proceedings of the IEEE International Conference on Robotics and Automation (ICRA), Hong Kong, China, 31 May–7 June 2014; pp. 119–125.
15. Vatsal, V.; Hoffman, G. At Arm's Length: Challenges in Building a Wearable Robotic Forearm for Human-Robot Collaboration. In Proceedings of the IEEE International Conference on Human Robot Interaction 2018, Chicago, IL, USA, 5–8 March 2018; pp. 271–272.
16. Saraiji, M.H.D.Y.; Sasaki, T.; Matsumura, R.; Minamizawa, K.; Inami, M. Fusion Full Body Surrogacy for Collaborative Communication. In Proceedings of the SIGGRAPH Emerging Technologies 2018, Vancouver, BC, Canada, 12–16 August 2018.
17. Sasaki, T.; Saraiji, M.H.D.Y.; Fernando, C.L.; Minamizawa, K.; Inami, M. MetaLimbs: Multiple Arms Interaction Metamorphism. In Proceedings of the SIGGRAPH Emerging Technologies 2017, Los Angeles, CA, USA, 30 July–3 August 2017.
18. Tanaka, H.; Yoshikawa, M.; Oyama, E.; Wakita, Y.; Matsumoto, Y. Development of Assistive Robots Using International Classification of Functioning, Disability, and Health: Concept, Applications, and Issues. *J. Robot.* **2013**, *2013*, 608191.
19. Bedirhan, ÜT.; Chatterji, S.; Bickenbach, J.; Kostanjsek, N.; Schneider, M. The International Classification of Functioning, Disability and Health: A New Tool for Understanding Disability and Health. *Disabil. Rehabil.* **2003**, *25*, 565–571.
20. Nakabayashi, K.; Iwasaki, Y.; Iwata, H. Development of Evaluation Indexes for Human-Centered Design of a Wearable Robot Arm. In Proceedings of the International Conference on Human Agent Interaction (HAI), Bielefeld, Germany, 17–20 October 2017.
21. HQL Database for Human Life Engineering. Available online: https://www.hql.jp/database/ (accessed on 15 September 2021).
22. National Institute of Advanced Industrial Science and Technology (AIST), AIST/HQL 3D Anthropometric Database 2003: Definitions of Measurement. Available online: https://www.airc.aist.go.jp/ (accessed on 15 September 2021).
23. Madinei, S.; Ning, X. Effects of the Weight Configuration of Hand Load on Trunk Musculature During Static Weight Holding. *Ergonomics* **2018**, *61*, 831–838.
24. Lloyd, R.; Parr, B.; Davies, S.; Cooke, C. A Kinetic Comparison of Back-loading and Headloading in Xhosa Women. *Ergonomics* **2011**, *54*, 380–391.
25. Anderson, A.M.; Meador, K.A.; McClure, L.R.; Makrozahopoulos, D.; Brooks, D.J.; Mirka, G.A. A Biomechanical Analysis of Anterior Load Carriage. *J. Ergon.* **2007**, *50*, 2104–2117.
26. Abe, D.; Muraki, S.; Yasukouchi, A. Ergonomic Effects of Load Carriage on the Upper and Lower Back Onmetabolic Energy Cost of Walking. *Appl. Ergon.* **2008**, *39*, 392–398.